March 9, 2023

Stay or Go: Sulfolobales Biofilm Dispersal is Dependent on a Bifunctional VapB Antitoxin

April M. Lewis[1], Daniel J. Willard[1], Mohammad J.H. Manesh[1], Shamphavi Sivabalasarma[2,3], Sonja-Verena Albers[2,3,4], and Robert M. Kelly[1*]

[1]Department of Chemical and Biomolecular Engineering, North Carolina State University, Raleigh, North Carolina, USA 27695-7905

[2]Institute for Biology, Molecular Biology of Archaea, University of Freiburg, 79104 Freiburg, Germany

[3]Spemann Graduate School of Biology and Medicine, University of Freiburg, Freiburg, Germany

[4]Signalling Research Centres BIOSS and CIBBS, Faculty of Biology, University of Freiburg, Freiburg, Germany

Submitted to: *mBio* (January 2023)

Keywords: Toxin-Antitoxin loci, biofilms, Sulfolobales, thermoacidophiles

Running Title: VapB Antitoxin regulates biofilm dispersal in the Sulfolobales

***Address Correspondence to:** Robert M. Kelly
Department of Chemical and Biomolecular Engineering
North Carolina State University
Raleigh, NC 27695
Phone: 919-515-6396
Email: rmkelly@ncsu.edu

Abstract

A Type II VapB14 Antitoxin regulates biofilm dispersal in the archaeal thermoacidophile *Sulfolobus acidocaldarius*, through traditional Toxin neutralization but also through noncanonical transcriptional regulation. Type II VapC Toxins are ribonucleases that are neutralized by their proteinaceous cognate Type II VapB Antitoxin. VapB Antitoxins have a flexible tail at their C-terminus that covers the Toxin's active site neutralizing its activity. VapB Antitoxins also have a DNA binding domain at their N-terminus that allows them to not only auto-repress their own promoters but also distal targets. VapB14 Antitoxin gene deletion in *S. acidocaldarius* stunted biofilm and planktonic growth and increased motility structures (archaella). Conversely, planktonic cells were devoid of archaella in the *ΔvapC14* cognate Toxin mutant. VapB14 is highly conserved at both the nucleotide and amino acid levels across the Sulfolobales, extremely unusual for Type II Antitoxins that are typically acquired through horizontal gene transfer. Furthermore, homologs of VapB14 are found across the Crenarchaeota, in some Euryarchaeota, and even bacteria. *S. acidocaldarius vapB14* and its homolog in the thermoacidophile *Metallosphaera sedula* (Msed_0871) were both up-regulated in biofilm cells, supporting the role of the Antitoxin in biofilm regulation. In several Sulfolobales species, including *M. sedula,* homologs of *vapB14* and *vapC14* are not co-localized. Strikingly, *Sulfuracidifex tepidarius* has an unpaired VapB14 homolog and lacks a cognate VapC14, illustrating the Toxin-independent conservation of the VapB14 Antitoxin. The findings here suggest that a stand-alone VapB-type Antitoxin was the product of selective evolutionary pressure to influence biofilm formation in these archaea, a vital microbial community behavior.

Importance

Biofilms allow microbes to resist a multitude of stresses and stay proximate to vital nutrients. The mechanisms of entering and leaving a biofilm are highly regulated to ensure microbial survival, but are not yet well described in archaea. Here, a VapBC Type II Toxin-Antitoxin system in the thermoacidophilic archaeon *Sulfolobus acidocaldarius* was shown to control biofilm dispersal through a multifaceted regulation of the archaeal motility structure, the archaellum. The VapC14 Toxin degrades an RNA that causes an increase in archaella and swimming. The VapB14 Antitoxin decreases archaella and biofilm dispersal by binding the VapC14 Toxin and neutralizing its activity, while also repressing the archaellum genes. VapB14-like Antitoxins are highly conserved across the Sulfolobales and respond similarly to biofilm growth. In fact, VapB14-like Antitoxins are also found in other archaea, and even in bacteria, indicating an evolutionary pressure to maintain this protein and its role in biofilm formation.

Introduction

Billions of years ago, prokaryotic organisms developed the ability to form biofilms (1), largely beneficial multi-cellular communities that confer resistance to stressors and aid in nutrient sequestration. Archaeal biofilms have been studied most intently in the Sulfolobales, particularly *Sulfolobus acidocaldarius, Saccharolobus solfataricus* (f. *Sulfolobus solfataricus*), and *Sulfurisphaera tokodaii* (f. *Sulfolobus tokodaii*), that have varying abilities to form biofilms despite similar extracellular polysaccharide matrix makeup (2). Some thermoacidophiles can form biofilms on sulfur (*Sulfuracidifex metallicus* (f. *Sulfolobus metallicus*) (3)) and iron pyrite (*Sulfu. metallicus* and *Acidianus spp.* (4)), substrates that serve as energy sources. There are three major phases of biofilm formation: attachment, maturation, and dispersal. In archaeal biofilms, attachment is typically mediated by type IV pili, proteinaceous structures that irreversibly adhere to surfaces and attach to other cells (5). *S. acidocaldarius* has three different type IV pili or type IV pili-like appendages: the Archaeal Adhesive Pili (Aap) (6), the situational UV-inducible pili (Ups) (7), and the primary motility appendage (the archaeal flagellum), referred to as the archaellum (6, 8). *S. acidocaldarius* primarily attaches to surfaces by the Aap pilus, although removal of the UV-inducible pili also has an acute effect on biofilm morphology (6). During maturation, attached cells produce an extracellular matrix consisting of polysaccharides, protein, lipids, and extracellular DNA (eDNA) (9). *S. acidocaldarius, Sa. solfataricus,* and *Sulfu. tokodaii* have extracellular matrices composed of polysaccharides containing glucose, galactose, mannose, and N-acetylglucosamine (2, 10), with protein structures and some eDNA also detected in *S. acidocaldarius* biofilms (11). Archaeal biofilm dispersal is mediated by the archaellum (6, 8), which propels cells to new locations potentially to form biofilm through reversible interactions with the substratum. In fact, deletion of the archaellum in *S. acidocaldarius* (6) leads to attachment defects.

Control of biofilm formation in *S. acidocaldarius* is accomplished by several known regulators. The one component system, ArnR (archaellar regulatory network regulator), and its

homolog, ArnR1, both act as activators of archaella by directly binding to the *arlB* gene promoter during nitrogen starvation (12). However, only ArnR binds to the promoter regions and directly induces expression of both *aapF* and *upsX* pili genes (12, 13). Additionally, the leucine-responsive regulator (Lrs) 14-like proteins of *S. acidocaldarius*, encoded by Saci_1223 and Saci_1242, are biofilm activators and result in an impaired biofilm upon deletion (14). Moreover, archaeal biofilm regulator 1 (AbfR1), another Lrs14-like regulator, is a known repressor of biofilm formation that, depending on its phosphorylation state, directly binds to *aap* and *arl* (archaellum genes) promoters (15). Deletion mutants of *abfR1* down-regulate *arl* genes, leading to decreased motility, and up-regulate *aap* genes, causing increased biofilm formation (14).

Beyond these mechanisms, other factors that regulate this phenomenon remain unknown. In mesophilic bacteria, Toxin-Antitoxin (TA) loci have been connected to biofilm formation. Type II TAs are most prevalent and consist of a Toxin protein that typically functions as a ribonuclease and an Antitoxin protein (16). The Antitoxin possesses a C-terminus that obstructs the Toxin active site, neutralizing its ribonuclease activity, and a DNA-binding N-terminus that autoregulates the TA operon (16-20). In several mesophilic bacteria, perturbing native TA systems leads to defects in biofilm formation. Deletion of TA systems in *Escherichia coli* caused defects in quorum sensing and biofilm attachment (21, 22), and stunted biofilm formation was observed in TA mutants of *Vibrio cholera* (23) and *S. pneumoniae* (24). In *Staphylococcus aureus,* deletion of *mazF* Type II Toxin gene also caused increased biofilm formation and higher sensitivity to antibiotic treatment (25). In *Caulobacter crescentus*, a $ParDE_4$ TA system is activated upon O_2 limitation and enhances eDNA stimulated dispersal from its biofilm, perhaps to seek out a more favorable situation (26). Interestingly, the Antitoxin's DNA-binding domain not only binds to its own promoter region, particularly when complexed with its cognate Toxin (27, 28), but can also bind to and regulate distal promoters (22, 29, 30). For example, the *E. coli* Type II Antitoxin MqsA, represses its own operon and that of the noncognate *cspD* Toxin (22). Additionally, MqsA represses the *rpoS* stress response sigma

120 factor that reduces the level of cyclic-di-GMP, causing an increase in motility and decrease in
121 biofilm (29). Moreover, all mutants of the *Pseudomonas putida mqsRA* Toxin-Antitoxin locus
122 showed significant biofilm defects. Not only did TA systems promote *P. putida* biofilm formation,
123 but the Antitoxin MqsA represses a sigma factor and a universal stress protein (30), illustrating
124 the Antitoxin's dual role of Toxin neutralizer and transcriptional regulator.

125 Much less is known about the function of TA systems in the Archaea. Studies have
126 shown that TA systems play a role in the heat shock response of *Sa. solfataricus* (31, 32) and
127 the response of *Metallosphaera spp.* to uranium exposure (33, 34). TA systems were
128 transcriptionally up-regulated in the thermoacidophile *Sa. solfataricus* during heat shock and
129 deletion of the *vapB6* Antitoxin gene resulted in a heat labile mutant (31). Furthermore,
130 *Metallosphaera prunae* developed resistance to hexavalent uranium, more so than its close
131 relative *Metallosphaera sedula*, by degrading its own cellular RNA via Toxin ribonucleases,
132 resulting in growth arrest and entry into a dormant state (33, 34).

133 Currently, the Toxin ribonuclease component of Type II TA systems has attracted the
134 most attention. Rarely have separate Antitoxin mutants been examined and, in fewer cases, has
135 the regulatory ability of the Antitoxin been investigated outside of its own operon. Furthermore,
136 Toxin-Antitoxin systems are often acquired through horizontal gene transfer leading to a lack of
137 nucleotide identity conservation, even within a species (35). Here, we focus on an archaeal
138 Type II Antitoxin's regulatory function beyond its own promoter, in which a VapB Antitoxin had a
139 profound effect on biofilm formation in *S. acidocaldarius*. The nucleotide identity of this Antitoxin,
140 VapB14, was highly conserved across the Sulfolobales and responded similarly to biofilm
141 growth in *M. sedula*, suggesting a significant role in regulating this phenomenon across the
142 Sulfolobales.
143

Results

Sulfolobus acidocaldarius biofilm transcriptome

Transcriptomics comparing biofilm to planktonic *S. acidocaldarius* cells identified genes associated with biofilm formation. Among the most biofilm-responsive genes was Saci_2184 that increased 10.8-fold in the biofilm compared to planktonic culture, second only to the hypothetical protein Saci_0301 (**Table 1**). The high transcriptional response of Saci_0301 was previously reported and its deletion causes a biofilm defect, which was found to be regulated by a non-coding RNA RrrR (RNase R resistant RNA) (36). Saci_2184 and Saci_2183 encode a putative VapB Type II Antitoxin and its cognate VapC Toxin, respectively. Using TAfinder (37), seventeen Type II Toxin-Antitoxin pairs are predicted in the *S. acidocaldarius* genome (**Fig. S1, Table 2**). The clustering of TA loci in the genome indicates a possible horizontal inheritance by mobile genetic elements (**Fig. S1**). Of these 17 potential TA pairs, two sets, Saci_1957/Saci_1956 and Saci_2111/Saci_2112, are not associated with any TA type and have predicted Toxins of an abnormally long length, suggesting they are unlikely to be Type II TAs. One identified TA pair was predicted as an MNT/HEPN-like system, which is common to thermophiles (38). MNT (minimal nucleotidyltransferase)-type Antitoxins inactivate their cognate HEPN (higher eukaryotes and prokaryotes nucleotide-binding) ribonucleases by AMPylation (39). Remaining TAs were identified as the VapBC type, including Saci_2184 (referred to here as VapB14). Interestingly, the VapB14 predicted cognate VapC-type Toxin Saci_2183 (referred to here as VapC14), was unresponsive in biofilm cells. In fact, except for *vapB14*, all other identified Toxin or Antitoxin genes were largely unresponsive in the biofilm (**Table 1**). All Toxin and Antitoxin genes, including *vapB14,* were between the 25th and 75th percentile of the transcriptome profile for both the biofilm and the planktonic condition. Follow-up relative quantitative real-time polymerase chain reaction (qPCR) analysis of *S. acidocaldarius* MW001 biofilm and planktonic cultures revealed a significant 2.2-fold increase in *vapB14* expression in the biofilm condition on day 3 (**Fig. 1A**), confirming these results. Moreover, *vapB14* is up-

regulated 2.9-fold in Saci_1223 (biofilm activator) mutant planktonic cells compared to the parent, suggesting that Saci_1223 is a repressor *vapB14* in planktonic growth (**Table 3**).

Reduction of VapC14 Toxin activity by its cognate VapB14 Antitoxin

The VapC14 Toxin and the VapB14 Antitoxin were recombinantly expressed and tested for their associated activities. Purified fractions of the VapC14 Toxin had a pinkish hue and correlated with the ~25 kDa VapC14 Toxin band on an SDS-PAGE gel (**Fig. S2**). This coloration in VapC14 containing fractions may be due to the co-elution of manganese ions, pinkish in aqueous solutions, that crystal structure studies indicate are present within VapC-type Toxin active sites (17, 18). Additionally, significant ribonuclease activity was measured in 5 µg of the VapC14 compared to the no protein control, confirming its function as an RNase-type Toxin (**Fig. 1B, S3**). No ribonuclease activity was measured in the VapB14 Antitoxin alone and the VapC14 Toxin's activity was completely abolished by the addition of the metal ion chelating agent, EDTA (**Fig. S3**). Addition of 10 µg of the VapB14 Antitoxin led to a mild 15% reduction in detectable VapC14 Toxin activity. However, VapC14 ribonuclease activity was significantly reduced with the addition of 20 µg (34%) and 30 µg (30%) of VapB14, confirming the Antitoxin function of VapB14 (**Fig. 1B**).

Regulation of the vapBC14 locus

Type II Toxin-Antitoxin systems are typically organized in an operon with the Antitoxin upstream and overlapping the Toxin or separated by a small intergenic region (35). This paradigm also applies to the *vapBC14* locus as the *vapB14* Antitoxin gene is upstream of the *vapC14* gene with only a 25 bp intergenic region. Often Type II Antitoxins auto-repress their own operon in conjunction with their cognate Toxin through a process called conditional cooperativity; repression of the operon is dependent on the ratio of Toxin:Antitoxin in the regulating TA complex (27, 28). If the ratio is skewed toward Antitoxin binding, repression

occurs; if the ratio is skewed toward Toxin, repression is relieved. If auto-repression was the only impact on the expression of the *vapBC14* locus, then deletion of the *vapB14* Antitoxin gene would cause an increase in the transcription of *vapC14.* However, qPCR showed a significant 5.7-fold decrease in *vapC14* expression in the *ΔvapB14* mutant compared to the MW001 parent strain in planktonic cultures (**Fig. 1C**), indicating the VapB14 Antitoxin may not be regulating the *vapC14* promoter, as predicted.

Role of the VapB14 Antitoxin in planktonic and biofilm growth

Single and double deletion mutants were generated for the *vapBC14* locus and continuous monitoring of planktonic cultures was performed to determine culture fitness (**Fig. 1D**). The *ΔvapBC14* Toxin-Antitoxin mutant and the *ΔvapC14* Toxin mutant grew similarly to the MW001 parent strain. However, planktonic growth of the *ΔvapB14* Antitoxin mutant exhibited a significant growth defect compared to any other strain at 48 and 72 h (**Fig. 1D**), 14% and 36% less than MW001, respectively. Neither the *ΔvapC14* Toxin nor the *ΔvapBC14* Toxin-Antitoxin mutants were significantly different from the parent at any time point. Additionally, *vapB14* expression increased a significant 2.6-fold in MW001 day 4 compared to day 1 planktonic cultures, indicating this Antitoxin may also play a role in late stationary phase growth (**Fig. 1A**).

Using crystal violet staining, a *vapBC14* mutant panel was evaluated for their ability to generate biofilms. Both the *ΔvapC14* Toxin and the *ΔvapBC14* Toxin-Antitoxin mutant were biofilm overproducers compared to the MW001 parent generating 47% and 65% more biofilm on day 3, and 124% and 119% more biofilm on day 4, respectively (**Fig. 2B, D**). The *ΔvapB14* Antitoxin mutant was deficient in biofilm growth compared to the MW001 parent strain at every time point, with a significant difference on days 1-3 (**Fig. 2B**). Even accounting for the *ΔvapB14* Antitoxin mutant's growth defect by normalizing the biofilm data to the overall growth of the well (OD_{600}), the *ΔvapB14* Antitoxin mutant retained a significant biofilm growth defect on days 2

(47% decrease) and day 3 (37% decrease) (**Fig. 2C**). The VapB14 Antitoxin may act as an activator of biofilm formation by regulating genes such as *abfr1*, which encodes a *S. acidocaldarius* biofilm repressor, but more evidence is needed to support this possibility. The biofilm defect seen in the *ΔvapB14* Antitoxin mutant could be due to the unfettered VapC14 Toxin targeting important biofilm RNAs, such as the transcript of the known Lrs14-like biofilm activator (Saci_1223).

Response of known biofilm genes to absence of the VapB14 Antitoxin

Response of known biofilm genes in the *ΔvapB14* Antitoxin mutant was determined via qPCR on 3-day-old biofilm and planktonic samples. The biofilm repressor *abfR1,* Saci_1242 biofilm activator, and UV-inducible pilus genes (*upsE* and *upsA*) registered no response to deletion of the *vapB14* Antitoxin gene in any conditions tested (**Fig. S4**). Strikingly, a 3-fold significant increase was observed in both *arlB* and *arlX* archaellum genes in the *ΔvapB14* Antitoxin mutant biofilm condition (**Fig. 3A-B**). Up-regulation of the archaellum in the *ΔvapB14* biofilm, which triggers dispersal from the biofilm, is consistent with the crystal violet experiments showing the *ΔvapB14* mutant produces significantly less biofilm. Furthermore, a slight increase was observed in both archaellum genes in the *ΔvapBC14* double mutant, but no such increase was seen in the *ΔvapC14* single mutant, indicating the importance of the VapB14 Antitoxin alone in the regulation of *S. acidocaldarius* motility. The VapB14 Antitoxin directly or indirectly represses the expression of key archaellum genes to minimize biofilm dispersal.

Additionally, the deletion of *vapC14* Toxin gene caused transcription of the *aapA* to be completely abolished in planktonic and biofilm cells, indicating that VapC14 Toxin targets an *aapA* repressor such as AbfR1 (**Fig. 3C**). However, the binding of AbfR1 is dependent on its phosphorylation state that differs across these conditions (15); relieving RNase degradation of *abfR1* transcript would not result in complete abrogation of the *aapA* transcription in both

247 planktonic and biofilm cells, as seen here. VapC14 is likely targeting an unknown repressor of
248 *aapA.*

249 Deletion of the *vapC14* Toxin, with or without the presence of the VapB14 Antitoxin,
250 caused a significant increase in *aapF* in planktonic cells (3.4-fold in *ΔvapC14*, 4.4-fold in
251 *ΔvapBC14*) compared to the MW001 parent (**Fig. 3D**). Antisense RNA transcripts are known to
252 be within the *Sa. solfataricus aapF* homolog (Sso_2386) (40) and deletion of the *aapF* in *S.*
253 *acidocaldarius* causes hyperarchaellation (41), which suggests that potential non-coding RNAs
254 within the *aapF* gene may repress archaellum expression. Increase in *aapF* transcription in only
255 *ΔvapC14* Toxin mutants indicates that the VapC14 Toxin targets either *aapF* mRNA or these
256 antisense transcripts, allowing them to accumulate in its absence. No significant change in *aapF*
257 was measured in the *ΔvapB14* Antitoxin mutant in either condition most likely due to the direct
258 repression of *aapF* by AbfR1 in biofilm cells (14) and the low expression of *vapB14* in planktonic
259 cells (**Table 1**).

260

261 *VapBC14 regulation of S. acidocaldarius surface structures*

262 Electron microscopy of 4-day biofilms showed hyperarchaellation of the *ΔvapB14*
263 Antitoxin mutant compared to the MW001 parent and *ΔvapC14* Toxin mutant (**Fig. 4C**).
264 Moreover, an increase in archaella was also detected in the *ΔvapB14* Antitoxin mutant biofilm
265 compared to any other strain via western blot using Anti-ArlB antibodies (**Fig. 4A-B**). EM
266 imaging and western blot of the *ΔvapBC14* Toxin-Antitoxin mutant biofilm displayed higher
267 levels of archaella than the MW001 parent (**Fig. 4A-C**), further confirming the Toxin-
268 independent role of the VapB14 Antitoxin in the regulation of *S. acidocaldarius* dispersal.
269 Additionally, both the *ΔvapC14* Toxin single mutant and the *ΔvapBC14* double mutant lacked
270 Aap pili structures, confirming qPCR results, and indicating that the VapC14 Toxin is a strong
271 regulator of Aap pili production. Furthermore, *ΔvapC14* Toxin mutant 4-day planktonic cultures
272 were devoid of most surface appendages, supporting the VapC14 Toxin's regulation of Aap pili

and archaella in planktonic cells. Thin structures referred to as “threads”, which are structurally similar to Type I pili (42), were unaffected by the VapBC14 TA system as they were seen in every strain at similar levels. However, the *ΔvapBC14* double mutant biofilm was hyperpiliated with Ups pili and hyperarchaellated in planktonic culture, which may be stress responses to the loss of other surface appendage structures. (**Fig. 4C**).

VapB14 Antitoxin homologs across the Sulfolobales and beyond

It was surprising to find that removal of VapB14, comprised of 114 amino acids, had such a profound impact on growth physiology and biofilm formation processes in *S. acidocaldarius*. This raises the question of whether homologous Antitoxins with similar roles exist in other Sulfolobales. In fact, homologs were identified in many Sulfolobales species (**Fig. 5A**). Interestingly, all surveyed species had at least one homolog of the VapB14 Antitoxin except for *Acidianus brierleyi, Acidianus infernus, Stygiolobus azoricus,* and *Sulfuracidifex metallicus*. *Metallosphaera yellowstonensis* was the only species with two *vapB14* homologs. Conversely, weaker homologs of the VapC14 Toxin were found in several Sulfolobales species with a much lower amino acid % identity (**Table 4**). Additionally, synteny analysis using the SyntTax webtool (43) identified several species that contained homologous VapB14 proteins that were not co-localized with the VapC14 Toxin gene. Sulfolobales species that have unpaired *vapB14* homologs include several members of the *Metallosphaera* species (*Metallosphaera hakonensis, Metallosphaera javensis, Metallosphaera prunae, Metalosphaera sedula,* and *Metallosphaera tengchongensis*), *Sulfodiicoccus acidiphilus,* and *Sulfuracidifex tepidarius*. In fact, despite the conservation of a VapB14 homolog (**Fig. 5A**), a VapC14 homolog is absent from the genome of *Sulfu. tepidarius* (**Table 4**). This suggests that the role of the VapB14 Antitoxin in biofilm development may be conserved among the Sulfolobales and less dependent on the conservation of its cognate Toxin. To this point, the transcriptional response of the *vapB14* homolog in *Metallosphaera sedula,* Msed_0871, in 3-day old biofilms and planktonic

cultures was consistent with the response of *vapB14* in *S. acidocaldrius* (**Fig. 5B**). Since *M. sedula* Msed_0871 is among the lowest homologies found among the Sulfolobales, other *vapB14* homologs with higher similarity likely also play a role in biofilm regulation. Moreover, *M. sedula* does possess both a *vapB14* Antitoxin (**Fig. 5A**) and a *vapC14* Toxin homolog (**Table 4**) but they are located at disparate locations in the genome, suggesting divergent functions.

Toxin-Antitoxin systems are often associated with mobile genetic elements and are highly susceptible to horizontal gene transfer between species (35). Because of the inherent mobility of these TA systems, it is common to see a large divergence in nucleotide identity even within the same species (35). However, VapB14 homologs across the Sulfolobales have conserved amino acid and nucleotide sequences (**Fig. 5A**). Furthermore, VapB14 homologs may be pivotal to regulating motility in Archaea as BlastP results shows VapB14 homologs in many members of the Phylum Crenarchaeota and some examples in the Euryarchaeota. Homologs were even identified in motile mesophilic bacterial genera, such as the pathogenic mesophiles of *Pseudomonas* and marine bacteria of *Nitrosococcus* (**Supplemental File 1**). While VapB14 clearly has an important role in the regulation of motility and its homologs are found in many motile prokaryotic species, this Antitoxin is also present in many non-motile genera, such as *Acidianus* of the Sulfolobales, thermophilic bacteria of *Thermoflexus*, and the mesophiles of *Gardneralla* (**Supplemental File 1**). VapB14, though important for regulation of the biofilm in the Sulfolobales through controlling dispersal, may have another regulatory role in non-motile species, such as biofilm attachment.

Discussion

The functional study of Toxin-Antitoxin systems remains controversial with recent investigations suggesting no phenotypic response to stressors despite a measured transcriptional response (44). However, this study identifies a VapC14 Toxin that significantly impacts RNA transcripts contained in the *aapF* gene, and the production of archaella and Aap

pili structures. Additionally, VapC14 RNase activity, though not completely abolished, was significantly reduced by its cognate Antitoxin, VapB14, confirming the canonical function of VapB14 as a VapC14 neutralizing Antitoxin. However, deletion of *vapB14* did not cause the expected upregulation of the *vapC14* Toxin gene and may indicate a third-party regulator of the *vapBC14* operon, which has some precedence (45, 46). Saci_1223 is a potential candidate as its deletion results in up-regulation of *vapB14* in planktonic cells. Deletion of *vapB14* could result in downstream polar effects, however, removal of *vapB14* left no genetic scar, minimizing the potential of this deleterious effect. Furthermore, RNase assays were performed *in vitro* and may not have been representative of the native conditions inside the cell which could lead to stronger affinity of the VapB14 Antitoxin for the VapC14 Toxin. Also, Antitoxins can be promiscuous, meaning that another Antitoxin may aid in the reduction of VapC14 RNase activity and that VapB14 may bind a second Toxin. The VapC14 Toxin's activity was lower than previously seen for VapC-type Toxin's in *M. sedula* (34). This lower activity could be due to a higher specificity for a very narrow range of transcripts, such as *aapF*, that may not be well represented in the RNA probes available in the kit used for measuring ribonuclease activity. Overall, RNase activity data demonstrated that VapC14 is a ribonuclease-type Toxin and that VapB14 does function as the Antitoxin to this activity (**Fig. 1B**).

The VapC14 Toxin most likely activates attachment by targeting a strong repressor of the *aapA* archaeal adhesive pilus structural subunit. This is further supported by the complete lack of pili structures in the *ΔvapC14* and *ΔvapBC14* mutants (**Fig. 4C**). However, these same mutants also are biofilm over-producers, which suggests they are employing an alternative attachment mechanism. Threads, the only non-type IV pilus surface filament on *S. acidocaldarius*, are present in EM images of all strains. Although the function of threads is still unknown, *S. acidocaldarius* Ups pili, Aap pili, and archaella triple mutants are capable of making biofilm (6). Threads may be playing a compensatory attachment role in the *ΔvapC14* and *ΔvapBC14* mutants, allowing these strains to produce biofilm. Similarly, the Ups hyperpiliation of

the *ΔvapBC14* double mutant may also improve its biofilm production (**Fig. 4C**). The *ΔvapBC14* double mutant biofilm also had an increase in archaella compared to the parent which could contribute to biofilm formation as archaella can aid in initial attachment (6, 47). Finally, *S. acidocaldarius aapX* and *aapE* mutants produce more extracellular matrix, which would contribute to biofilm formation (41). As there were no visible pili in the *ΔvapC14* single or *ΔvapBC14* double mutant (**Fig. 4C**), it is reasonable to assume that AapX and AapE are absent in these strains yielding excess extracellular matrix. Overall, ΔvapC14 Toxin and ΔvapBC14 double mutants may be biofilm over-producers through alternative attachment mechanisms and overexpression of extracellular matrix.

Additionally, in planktonic cells, *aapF* is significantly increased in the absence of the VapC14 Toxin (**Fig. 3D**), which may contain antisense non-coding RNAs like those observed in the *Sa. solfataricus aapF* homolog (40). Furthermore, deletion of *aapF* in *S. acidocaldarius* causes an increase in archaella (41), suggesting that AapF or potential non-coding transcripts within the *aapF* gene repress archaella expression. An abundance of antisense *aapF* transcript may function as non-coding RNAs that post-transcriptionally down regulate archaellum gene expression. As is natural for a Toxin-Antitoxin system, VapC14 and VapB14 may apply opposing regulatory pressure on archaellum expression. VapC14 derepresses the archaella by degrading *aapF* mRNA or a non-coding RNA during planktonic growth. However, during biofilm growth VapB14 is highly expressed and transcriptionally represses the archaellum. VapB14 also behaves as a traditional Antitoxin by neutralizing the VapC14 Toxin, allowing the archaellum to be post-transcriptionally repressed (**Fig. 6**). While nutrient starvation is known to induce expression of the archaellum in *S. acidocaldarius* (48) through regulation by ArnR (12), the VapBC14 TA system's regulation of the archaellum is responsive to biofilm growth rather than nutrient availability.

Unlike Bacteria, non-coding RNAs are plentiful in the genomes of Archaea (40). Since Archaea are lacking sigma factors and have an abundance of Type II Toxin-Antitoxin systems,

this may point to ribonuclease activity of Type II Toxins as an important regulatory mechanism within this domain. Specifically, homologs of both AapF and VapB14 are found in most surveyed Sulfolobales species (**Supplemental Results**, **Fig. S5**, **5A**), suggesting that the mechanism of archaellum regulation described here may be a multispecies phenomenon that is present in all archaellated Sulfolobales. This is further supported by the similar up-regulation of the *M. sedula* VapB14 homolog (Msed_0871) to biofilm growth (**Fig. 5B**). Additionally, conservation of *vapB14* is independent of *vapC14*, as several Sulfolobales species either encode these genes at distinct locations or possess only a *vapB14* Antitoxin gene. Moreover, VapB14 homologs are prevalent in the archaeal Phylum Crenarchaeota and present in some species of the Phylum Euryarchaeota (**Supplemental File 1**). While the importance of VapB14 in motile Archaea is evident, homologs are also found in some bacterial species and non-motile organisms, indicating that VapB14 may also have other functions.

TA systems are prevalent in bacteria, archaea, and fungi (16) suggesting that the evolution of the current Type II TA systems are not a recent occurrence. Fossil evidence has also shown that prokaryotic organisms of both bacterial and archaeal origin were forming multicellular biofilms more than 3 billion years ago (1). In fact, the earliest recorded occurrences of biofilms are in hydrothermal environments like those native to the species of the Sulfolobales (1). It is, therefore, possible that this VapBC14 TA system may have co-evolved with the ability to form a biofilm within this thermophilic order. Furthermore, nucleotide sequence conservation of a Type II TA system is atypical due to their association with mobile genetic elements and tendency toward horizontal gene transfer (35, 49). However, VapB14 is highly conserved across the Sulfolobales (**Fig. 5A**) indicating an evolutionary selective pressure to maintain this small but important biofilm regulating protein. Overall, the bifunctional VapB14 Antitoxin has evolved as an important regulator of Sulfolobales, and perhaps archaeal, motility by not only inhibiting the activity of its cognate Toxin but also through transcriptional repression of the archaellum (**Fig. 6**).

Materials and Methods

Ribonuclease activity assay

Ribonuclease activity assays were performed as described previously using the RNaseAlert® kit (Integrated DNA Technologies) (34). For each reaction containing VapC14, 5 µg of VapC14 Toxin was added with or without the addition of 10 µg, 20 µg or 30 µg of VapB14 Antitoxin, or 25 mM EDTA. A no protein and a 10 µg of VapB14 Antitoxin alone control were also performed. All reaction were prewarmed at 75°C for 5 min to activate the VapC14 Toxin and VapB14 Antitoxin.

Planktonic growth curves

Cultures were inoculated from frozen stocks in 50 mL 75°C prewarmed Brock's salts pH3 supplemented with 0.1% NZ-amine + 0.2% sucrose + 0.01g/L uracil. Cultures of *S. acidocaldarius* MW001, *ΔvapB14, ΔvapC14*, and *ΔvapBC14* were grown aerobically in foam stoppered flasks at a 1:5 volume to flask ratio at 75°C, 150 rpm. Cultures were monitored by backscatter at 520 nm every 15 min with the Cell Growth Quantifier (Scientific Bioprocessing, inc.) for 72 h.

Crystal violet biofilm assay

The *S. acidocaldarius* MW001 parent, *ΔvapB14* Antitoxin, *ΔvapC14* Toxin, and *ΔvapBC14* Toxin-Antitoxin mutant biofilms were grown in 1 mL of Brock's basal salts pH 3 + 0.1% NZ-amine + 0.2% sucrose + 0.01 g/L uracil on Sarstedt Cell^{+} flat bottom 24 well plates at 75°C for a period of 1 to 4 days. Outer wells of each 24 well plate were filled with 1 mL of water and plates were incubated in a humidified box to reduce evaporation. Prior to staining, optical density was read at 600 nm as a measure of overall well growth. Supernatant was then

removed, attached biofilm stained with 500 µL 0.1% crystal violet, washed twice with 1 mL of water, and crystal violet solubilized with 500 µL 100% ethanol and absorbance read at 550 nm.

RNA isolation and quantitative real-time polymerase chain reaction

S. acidocaldarius MW001 and mutant planktonic cultures were grown in 50 mL 75°C prewarmed Brock's salts pH3 supplemented with 0.1% NZ-amine + 0.2% sucrose + 0.01g/L uracil. Cultures were inoculated at an OD_{600} = 0.01 and grown aerobically in foam stoppered flasks at a 1:5 volume to flask ratio at 75°C, 150 rpm for 4 days. On day 2, 20 mL of sterile 75°C deionized water was added to each flask. The entire culture of cells was centrifuged at 4000 xg for 5 min and resuspended in 1 mL of RNAlater (Invitrogen). *S. acidocaldarius* MW001 and mutant biofilm cultures were inoculated in the same prewarmed medium at an OD_{600} = 0.01 in 150 x 20 mm Sarstedt Cell^{+} tissue culture dishes (Sarstedt). Biofilms were incubated at 75°C in a sealed humidified box for 4 days. RNA was then extracted on days 1-4 for the *S. acidocaldarius* MW001 and *ΔvapB14* Antitoxin mutant, and on day 3 for the *ΔvapC14* Toxin and *ΔvapBC14* double mutants using Trizol reagent followed by the RNA easy kit (Qiagen) (50). Residual DNA was removed with a rigorous treatment of Turbo DNase (Invitrogen). RNA was determined to be relatively free of DNA contamination by qPCR checking for amplification using *secY* primers (**Supplemental File 2**) with RNA as template. Relative qPCR was performed using SsoFast EvaGreen Supermix (Bio-Rad) or SsoAdvanced Universal SYBR® Green Supermix (Bio-Rad) and fold change values were calculated using the Livak method (51) with *secY* used as the normalizer.

M. sedula planktonic and biofilm cultures were inoculated as above with the following exceptions. Cultures were inoculated in 50 mL 70°C prewarmed Brock's salts pH2 supplemented with 0.1% yeast extract and incubate at 70°C, 150 rpm for planktonic cultures and 70°C stationary for biofilm plates for 3 days. RNA was determined to be relatively free of DNA contamination by qPCR checking for amplification using Msed_R0026 16s gene primers

(**Supplemental File 2**) with RNA as template. Relative qPCR was performed using SsoAdvanced Universal SYBR® Green Supermix (Bio-Rad) and fold change values were calculated using the Livak method (51) with Msed_R0026 used as the normalizer.

Transmission electron microscopy of S. acidocaldarius surface appendage structures

Biofilms and planktonic *S. acidocaldarius* MW001 and mutant strains were grown as for RNA isolation. Biofilm was scraped off the petri dishes and resuspended in 1 mL growth medium. 5 µL of biofilm or planktonic cells were applied on freshly glow-discharged carbon/formvar coated copper grids (300 mesh, Plano GmbH) and incubated for 30 seconds. The excess liquid was blotted away and cells were negatively stained with 2% Uranyl acetate. Imaging was done with Hitachi HT7800 operated at 100 kV, equipped with an EMSIS XAROSA 20 Megapixel CMOS camera.

Western blotting

To assay the production of ArlB in planktonic and biofilm *S. acidocaldarius* MW001 and mutant strains were grown as for RNA isolation. Biofilm was scraped off the petri dishes and resuspended in 1 mL growth medium. The OD_{600} of cells from biofilm and planktonic cultures were determined. Cells were pelleted at 2400 x g in a tabletop centrifuge for 10 min and resuspended to a theoretical OD of 10 in 1x SDS loading dye. The whole cell samples were separated on SDS-PAGE and blotted on PVDF membrane (Roche). The membrane was blocked with I-Block (Thermo Fisher Scientific) and incubated in primary antibody against ArlB (Eurogentec) overnight at 4°C. Afterwards, the membrane was incubated in secondary goat anti-rabbit antibody coupled to HRP overnight at 4°C. Chemiluminescent signals were recorded with IBright 1500 (Invitrogen, Thermo Fisher Scientific) using Clarity Western ECL blotting substrate (Bio-Rad).

Data Availability

Microarray data is available at Gene Expression Omnibus repository (NCBI) accession number GSE226483 for normalized data, and accession numbers GSM707782, GSM7077822, GSM7077823, GSM7077824 for raw data files.

Acknowledgments

This work was supported by the US Air Force Office of Scientific Research (FA9550-17-1-0268, FA9550-20-1-0216) and the US National Science Foundation (CBET-1802939). DJW acknowledges support from an NIH Biotechnology Traineeship (2T32GM008776). SS and SVA were supported by the Deutsche Forschungsgemeinschaft (German Research Foundation) under project no. 403222702-SFB 1381. We thank Arpan Mukherjee and Alvaro Orell for performing the microarray.

DJW created the get homologs database, MJH isolated RNA for qPCR, SS generated the western blot and EM images. AML performed the remaining experiments and wrote the original draft of the manuscript. All authors contributed to editing the manuscript.

References:

1. Hall-Stoodley L, Costerton JW, Stoodley P. 2004. Bacterial biofilms: from the natural environment to infectious diseases. Nat Rev Microbiol 2:95-108.
2. Koerdt A, Gödeke J, Berger J, Thormann KM, Albers SV. 2010. Crenarchaeal biofilm formation under extreme conditions. PLoS One 5:e14104.
3. Zhang R, Neu TR, Zhang Y, Bellenberg S, Kuhlicke U, Li Q, Sand W, Vera M. 2015. Visualization and analysis of EPS glycoconjugates of the thermoacidophilic archaeon *Sulfolobus metallicus*. Appl Microbiol Biot 99:7343-7356.
4. Castro C, Zhang R, Liu J, Bellenberg S, Neu TR, Donati E, Sand W, Vera M. 2016. Biofilm formation and interspecies interactions in mixed cultures of thermo-acidophilic archaea *Acidianus spp.* and *Sulfolobus metallicus*. Res Microbiol 167:604-612.
5. van Wolferen M, Orell A, Albers S-V. 2018. Archaeal biofilm formation. Nat Rev Microbiol 16:699-713.
6. Henche A-L, Koerdt A, Ghosh A, Albers S-V. 2012. Influence of cell surface structures on crenarchaeal biofilm formation using a thermostable green fluorescent protein. Environ Microbiol 14:779-793.
7. Schult F, Le TN, Albersmeier A, Rauch B, Blumenkamp P, van der Does C, Goesmann A, Kalinowski J, Albers S-V, Siebers B. 2018. Effect of UV irradiation on *Sulfolobus acidocaldarius* and involvement of the general transcription factor TFB3 in the early UV response. Nucleic Acids Res 46:7179-7192.
8. Jarrell KF, Albers S-V. 2012. The archaellum: an old motility structure with a new name. Trends in Microbiol 20:307-312.
9. Flemming H-C, Neu TR, Wozniak DJ. 2007. The EPS matrix: the “house of biofilm cells”. J Bacteriol 189:7945-7947.

10. Koerdt A, Jachlewski S, Ghosh A, Wingender J, Siebers B, Albers S-V. 2012. Complementation of *Sulfolobus solfataricus* PBL2025 with an α-mannosidase: effects on surface attachment and biofilm formation. Extremophiles 16:115-125.
11. Jachlewski S, Jachlewski WD, Linne U, Bräsen C, Wingender J, Siebers B. 2015. Isolation of extracellular polymeric substances from biofilms of the thermoacidophilic archaeon *Sulfolobus acidocaldarius*. Front Bioeng Biotechnol 3:123.
12. Lassak K, Peeters E, Wróbel S, Albers S-V. 2013. The one-component system ArnR: a membrane-bound activator of the crenarchaeal archaellum. Mol Microbiol 88:125-139.
13. Bischof LF, Haurat MF, Albers SV. 2019. Two membrane-bound transcription factors regulate expression of various type-IV-pili surface structures in. PeerJ 7:e6459.
14. Orell A, Peeters E, Vassen V, Jachlewski S, Schalles S, Siebers B, Albers S-V. 2013. Lrs14 transcriptional regulators influence biofilm formation and cell motility of Crenarchaea. ISME J 7:1886-1898.
15. Li L, Banerjee A, Bischof LF, Maklad HR, Hoffmann L, Henche AL, Veliz F, Bildl W, Schulte U, Orell A. 2017. Wing phosphorylation is a major functional determinant of the Lrs14-type biofilm and motility regulator AbfR1 in *Sulfolobus acidocaldarius*. Mol Microbiol 105:777-793.
16. Yamaguchi Y, Park JH, Inouye M. 2011. Toxin-antitoxin systems in bacteria and archaea. Annu Rev Genet 45:61-79.
17. Dienemann C, Bøggild A, Winther KS, Gerdes K, Brodersen DE. 2011. Crystal structure of the VapBC toxin–antitoxin complex from *Shigella flexneri* reveals a hetero-octameric DNA-binding assembly. J Mol Biol 414:713-722.
18. Das U, Pogenberg V, Subhramanyam UKT, Wilmanns M, Gourinath S, Srinivasan A. 2014. Crystal structure of the VapBC-15 complex from *Mycobacterium tuberculosis* reveals a two-metal ion dependent PIN-domain ribonuclease and a variable mode of toxin–antitoxin assembly. J Struct Biol 188:249-258.

19. Kang S-M, Jin C, Kim D-H, Lee Y, Lee B-J. 2020. Structural and functional study of the *Klebsiella pneumoniae* VapBC toxin–antitoxin system, including the development of an inhibitor that activates VapC. J Med Chem 63:13669-13679.
20. Deep A, Kaundal S, Agarwal S, Singh R, Thakur KG. 2017. Crystal structure of *Mycobacterium tuberculosis* VapC20 toxin and its interactions with cognate antitoxin, VapB20, suggest a model for toxin–antitoxin assembly. The FEBS J 284:4066-4082.
21. Kim Y, Wang X, Ma Q, Zhang X-S, Wood TK. 2009. Toxin-antitoxin systems in *Escherichia coli* influence biofilm formation through YjgK (TabA) and fimbriae. J Bacteriol 191:1258.
22. Kim Y, Wang X, Zhang X-S, Grigoriu S, Page R, Peti W, Wood TK. 2010. *Escherichia coli* toxin/antitoxin pair MqsR/MqsA regulate toxin CspD. Environ Microbiol 12:1105-1121.
23. Wang Y, Wang H, Hay AJ, Zhong Z, Zhu J, Kan B. 2015. Functional RelBE-family toxin-antitoxin pairs affect biofilm maturation and intestine colonization in *Vibrio cholerae*. PLoS ONE 10:e0135696.
24. Chan WT, Domenech M, Moreno-Córdoba I, Navarro-Martínez V, Nieto C, Moscoso M, García E, Espinosa M. 2018. The *Streptococcus pneumoniae yefM-yoeB* and *relBE* toxin-antitoxin operons participate in oxidative stress and biofilm formation. Toxins 10:378.
25. Ma D, Mandell JB, Donegan NP, Cheung AL, Ma W, Rothenberger S, Shanks RMQ, Richardson AR, Urish KL. 2019. The Toxin-Antitoxin MazEF Drives *Staphylococcus aureus* Biofilm Formation, Antibiotic Tolerance, and Chronic Infection. mBio 10.
26. Berne C, Zappa S, Brun YV. 2022. eDNA-stimulated cell dispersion from *Caulobacter crescentus* biofilms upon oxygen limitation is dependent on a toxin-antitoxin system. Elife 11:e80808.

572 27. Overgaard M, Borch J, Jørgensen MG, Gerdes K. 2008. Messenger RNA interferase
573 RelE controls *relBE* transcription by conditional cooperativity. Mol Microbiol 69:841-857.
574 28. Garcia-Pino A, Balasubramanian S, Wyns L, Gazit E, De Greve H, Magnuson RD,
575 Charlier D, van Nuland NA, Loris R. 2010. Allostery and intrinsic disorder mediate
576 transcription regulation by conditional cooperativity. Cell 142:101-111.
577 29. Wang X, Kim Y, Hong SH, Ma Q, Brown BL, Pu M, Tarone AM, Benedik MJ, Peti W,
578 Page R, Wood TK. 2011. Antitoxin MqsA helps mediate the bacterial general stress
579 response. Nat Chem Biol 7:359-66.
580 30. Sun C, Guo Y, Tang K, Wen Z, Li B, Zeng Z, Wang X. 2017. MqsR/MqsA Toxin/Antitoxin
581 System Regulates Persistence and Biofilm Formation in *Pseudomonas putida* KT2440.
582 Front Microbiol 8.
583 31. Cooper CR, Daugherty AJ, Tachdjian S, Blum PH, Kelly RM. 2009. Role of *vapBC* toxin–
584 antitoxin loci in the thermal stress response of *Sulfolobus solfataricus*. Biochem Soc T
585 37:123-126.
586 32. Cooper CR, Lewis AM, Notey JS, Mukherjee A, Willard DJ, Blum PH, Kelly RM. 2023.
587 Interplay between transcriptional regulators and VapBC toxin-antitoxin loci during
588 thermal stress response in extremely thermoacidophilic archaea. Environ Microbiol.
589 33. Mukherjee A, Wheaton GH, Blum PH, Kelly RM. 2012. Uranium extremophily is an
590 adaptive, rather than intrinsic, feature for extremely thermoacidophilic *Metallosphera*
591 *prunae*. P Natl Acad Sci USA 109:16702-16707.
592 34. Mukherjee A, Wheaton GH, Counts JA, Ijeomah B, Desai J, Kelly RM. 2017. VapC
593 toxins drive cellular dormancy under uranium stress for the extreme thermoacidophile
594 *Metallosphaera prunae*. Environ Microbiol 19:2831-2842.
595 35. Jurėnas D, Fraikin N, Goormaghtigh F, Van Melderen L. 2022. Biology and evolution of
596 bacterial toxin–antitoxin systems. Nat Rev Microbiol 20:335-350.

36. Orell A, Tripp V, Aliaga-Tobar V, Albers S-V, Maracaja-Coutinho V, Randau L. 2018. A regulatory RNA is involved in RNA duplex formation and biofilm regulation in *Sulfolobus acidocaldarius*. Nucleic Acids Res 46:4794-4806.

37. Microbial Bioinformatics Group in MML S. 2017. https://bioinfo-mml.sjtu.edu.cn/TAfinder/index.php. Accessed October.

38. Makarova KS, Wolf YI, Koonin EV. 2009. Comprehensive comparative-genomic analysis of type 2 toxin-antitoxin systems and related mobile stress response systems in prokaryotes. Biol Direct 4:1-38.

39. Songailiene I, Juozapaitis J, Tamulaitiene G, Ruksenaite A, Šulčius S, Sasnauskas G, Venclovas Č, Siksnys V. 2020. HEPN-MNT toxin-antitoxin system: the HEPN ribonuclease is neutralized by OligoAMPylation. Mol Cell 80:955-970. e7.

40. Wurtzel O, Sapra R, Chen F, Zhu Y, Simmons BA, Sorek R. 2010. A single-base resolution map of an archaeal transcriptome. Genome Res 20:133-141.

41. Henche AL, Ghosh A, Yu X, Jeske T, Egelman E, Albers SV. 2012. Structure and function of the adhesive type IV pilus of *Sulfolobus acidocaldarius*. Environ Microbiol 14:3188-3202.

42. Gaines MC, Isupov MN, Sivabalasarma S, Haque RU, McLaren M, Mollat CL, Tripp P, Neuhaus A, Gold VA, Albers S-V. 2022. Electron cryo-microscopy reveals the structure of the archaeal thread filament. Nat Commun 13:1-13.

43. Oberto J. 2013. SyntTax: a web server linking synteny to prokaryotic taxonomy. BMC Bioinform 14:1-10.

44. LeRoux M, Culviner PH, Liu YJ, Littlehale ML, Laub MT. 2020. Stress can induce transcription of toxin-antitoxin systems without activating toxin. Mol Cell 79:280-292.e8.

45. Hallez R, Geeraerts D, Sterckx Y, Mine N, Loris R, Van Melderen L. 2010. New toxins homologous to ParE belonging to three-component toxin–antitoxin systems in *Escherichia coli* O157: H7. Mol Microbiol 76:719-732.

623 46. Zielenkiewicz U, Cegłowski P. 2005. The toxin-antitoxin system of the streptococcal
624 plasmid pSM19035. J Bacteriol 187:6094-6105.
625 47. Näther DJ, Rachel R, Wanner G, Wirth R. 2006. Flagella of *Pyrococcus furiosus*:
626 multifunctional organelles, made for swimming, adhesion to various surfaces, and cell-
627 cell contacts. J Bacteriol 188:6915-6923.
628 48. Lassak K, Neiner T, Ghosh A, Klingl A, Wirth R, Albers S-V. 2012. Molecular analysis of
629 the crenarchaeal flagellum. Mol Microbiol 83:110-124.
630 49. LeRoux M, Laub MT. 2022. Toxin-Antitoxin Systems as Phage Defense Elements. Annu
631 Rev Microbiol 76.
632 50. Wheaton GH, Vitko NP, Counts JA, Dulkis JA, Podolsky I, Mukherjee A, Kelly RM. 2019.
633 Extremely Thermoacidophilic *Metallosphaera* Species Mediate Mobilization and
634 Oxidation of Vanadium and Molybdenum Oxides. Appl Environ Microbiol 85:e02805-18.
635 51. Livak KJ, Schmittgen TD. 2001. Analysis of relative gene expression data using real-
636 time quantitative PCR and the $2^{-\Delta\Delta CT}$ method. Methods 25:402-408.

FIGURE AND TABLE CAPTIONS

Figure 1. *S. acidocaldarius* VapBC14 expression and activity. **A)** Differential *vapB14* expression in *S. acidocaldarius* biofilm and planktonic cultures. Relative qPCR of total RNA isolated from *S. acidocaldarius* MW001 biofilm and planktonic cultures across four days of growth. Graphed data represents the average fold change of *vapB14* expression of n = 3 biological replicates compared to the day 1 planktonic condition ± standard error of the mean (SEM). Graphed points are the fold-change in individual biological replicates. *Statistically significant difference with a $p<0.05$. ** Statistically significant difference with a $p<0.01$ compared to the day 1 planktonic condition. **B)** Reduction of VapC14 RNase activity by VapB14 Antitoxin. N = 3 experimental replicates ± SEM. **Statistically significant difference from 5 µg VapC14 Toxin alone at 60 min with a $p<0.01$ or ● $p<0.10$. **C)** Differential *vapC14* expression in *S. acidocaldarius* MW001 and *ΔvapB14* mutant biofilm and planktonic cultures. Relative qPCR of total RNA isolated from *S. acidocaldarius* MW001 and *ΔvapB14* mutant biofilm and planktonic cultures after three days of growth. Graphed data represents the average fold change of *vapC14* expression of n = 3 biological replicates (n =4 for *ΔvapB14* mutant biofilm) compared to the MW001 parent planktonic condition ± SEM. Graphed points are the fold-change in individual biological replicates. *Statistically significant difference with a $p<0.05$. **D)** *S. acidocaldarius* MW001 parent, and *ΔvapB14*, *ΔvapC14*, and *ΔvapBC14* mutant planktonic growth curves monitored by backscatter at 520 nm. Each curve represents the average of n =4 independent experiments ± SEM. The *ΔvapB14* mutant is significantly different from the MW001 parent at ● 48 hr ($p<0.10$) and ** 72 hr ($p<0.05$). Statistical differences were calculated using a two-way analysis of variance (ANOVA) followed by a Tukey Honestly Significant Difference (Tukey HSD) post hoc test for panels A, B, and D, and a Dunnett T3 test for panel C.

Figure 2. *S. acidocaldarius vapBC14* locus impact on biofilm and planktonic growth. **A)** to **C)** MW001 parent strain, *ΔvapB14* Antitoxin mutant, *ΔvapC14* Toxin mutant, and *ΔvapBC14*

Toxin-Antitoxin mutant biofilm growth for a period of 1 to 4 days. Prior to staining, optical density was read at 600 nm as a measure of overall well growth. Crystal violet-stained biofilm absorbance was read at 550 nm as a measure of biofilm growth. Each graph represents a n=4 for each strain except for the MW001 parent, which has a n=8. **A)** Graph of average OD_{600} measurements of overall well growth ± SEM. **B)** Graph of average OD_{550} measurements of biofilm growth ± SEM. **C)** Graph of OD_{550}/OD_{600} average measurements of biofilm growth normalized to the overall growth of the well ± SEM. **D)** Image of crystal violet stained 4-day biofilms prior to solubilization. *Statistically significant difference with a $p<0.05$ compared to the MW001 parent within the same day. ● Statistically significant difference with a $p<0.10$ compared to the MW001 parent within the same day. All statistical differences were calculated using a two-way analysis of variance (ANOVA) followed by a Dunnett T3 test.

Figure 3. Effect of VapBC14 on the transcriptional expression of the *S. acidocaldarius* archaeal adhesive pilus and archaellum genes. Differential expression of archaellum genes, **A)** *arlB* and **B)** *arlX,* and archaeal adhesive pilus genes, **C)** *aapA* and **D)** *aapF* in *S. acidocaldarius* MW001 parent, *ΔvapB14* Antitoxin, *ΔvapC14* Toxin, and *ΔvapBC14* Antitoxin-Toxin mutant biofilm and planktonic cultures. Relative qPCR of total RNA isolated from biofilm and planktonic cultures after three days of growth. Graphed data represents the average fold change of each gene's expression of n = 3 biological replicates compared to the MW001 parent planktonic condition ± SEM. Graphed points are the fold-change in individual biological replicates. *Statistically significant difference with a $p<0.05$ compared to the MW001 parent in the same condition. N.D. = none detected as cycle threshold was above the detection limit. All statistical differences were calculated using a two-way analysis of variance (ANOVA) followed by a Tukey Honestly Significant Difference (Tukey HSD) post hoc test.

Figure 4. Effect of VapBC14 on *S. acidocaldarius* archaeal adhesive pilus and archaellum surface structures. A) Loading control and **B)** archaellum western blot using an Anti-ArlB antibody. **C)** Electron microscopy images of *S. acidocaldarius* MW001 parent, *ΔvapB14* Antitoxin, *ΔvapC14* Toxin, and *ΔvapBC14* Antitoxin-Toxin mutant biofilm and planktonic cells. Red arrows indicate archaella and blue arrows indicate Aap pili. Scale bar is 1 μm.

Figure 5 Sulfolobales VapB14 homolog conservation and biofilm response. A) Prevalence of VapB14 Antitoxin homologs in the Sulfulobales **B)** Differential expression of Msed_0871 *vapB14* homolog in *Metallosphaera sedula* biofilm and planktonic cultures. Relative qPCR of total RNA isolated from *M. sedula* biofilm and planktonic cultures after three days of growth. Graphed data represents the average fold change of Msed_0871 expression of n = 4 biological replicates compared to the planktonic condition ± SEM. Graphed points are the fold-change in individual biological replicates. *Statistically significant difference with a $p<0.05$ using a two-tailed student's t-test.

Figure 6. Archaellum regulation by the VapB14 Antitoxin and VapC14 Toxin. In planktonic conditions the VapC14 Toxin degrades *aapF* RNA transcripts relieving archaella repression and inducing motility. In biofilm conditions the VapB14 Antitoxin functions by both transcriptionally repressing the archaellum (*arl*) locus and suppressing the post-transcriptional degradation of the *aapF* transcript by the VapC14 Toxin leading to a down-regulation in motility and induction of biofilm formation.

Table 1. *Sulfolobus acidocaldarius vapBC* Transcriptional Response to Biofilm Formation.

Table 2. *Sulfolobus acidocaldarius* TAfinder Results.

Table 3. *Sulfolobus acidocaldarius vapBC14* Transcriptional Response to *saci_1223* Deletion

Table 4. Prevalence of VapC14 Toxin homologs in the Sulfolobales.

SUPPLEMENTAL MATERIAL

Figure S1. Location of identified Type II Toxin-Antitoxins in the *Sulfolobus acidocaldarius* genome.

Figure S2. Purification of the VapC14 Toxin. A) VapC14 Toxin purification chromatogram from VapBC14 co-expression. **B)** VapC14 Toxin purification fractions coloration and gel.

Figure S3. Ribonuclease activity of the VapC14 Toxin Reduction of VapC14 RNase activity by VapB14 Antitoxin. N =3 experimental replicates ± SEM. ** Statistically significant difference from the no protein control at 60 min with a $p<0.01$ calculated using a one-way analysis of variance (ANOVA) followed by a Tukey Honestly Significant Difference (Tukey HSD) post hoc test.

Figure S4. Differential expression of known biofilm genes in *S. acidocaldarius* MW001 parent and *ΔvapB14* mutant biofilm and planktonic cultures. Relative qPCR of total RNA isolated from *S. acidocaldarius* MW001 biofilm and planktonic cultures after three days of growth. Graphed data represents the average fold change of each gene's expression of n = 3

biological replicates compared to the MW001 parent planktonic condition ± SEM. Graphed points are the fold-change in individual biological replicates. Lack of statistical differences were calculated using a two-way analysis of variance (ANOVA) followed by a Tukey Honestly Significant Difference (Tukey HSD) post hoc test.

Figure S5. Prevalence of archaellum and Type IV Pili homologs in the Sulfolobales

Supplemental File S1. *Sulfolobus acidocaldarius* VapB14 BLASTP Results

Supplemental File 2. Primer, Plasmid, and Strain Tables

Supplemental File 3. Sulfolobales Biofilm Gene Homologs and Sulfolobus Pangenome

Table 1. *Sulfolobus acidocaldarius vapBC* Transcriptional Response to Biofilm Formation.

Gene Product	Gene ID	LSM Biofilm	% Rank Biofilm	LSM Planktonic	% Rank Planktonic	Difference Biofilm - Planktonic	Fold Change Biofilm - Planktonic	p-value
Hypothetical protein	Saci_0301	5.01	86.4	0.75	55.7	4.26	19.15	3.68E-22
NAD-dependent alcohol dehydrogenase	Saci_0557	5.51	90.2	6.71	100.0	1.12	-2.31	4.17E-12
DNA-directed RNA polymerase subunit P	Saci_0864	6.80	100.0	5.68	92.3	-1.21	-2.31	3.32E-07
VapC1	Saci_0467	-0.59	43.6	-0.22	48.6	-0.38	-1.30	7.39E-02
VapB1	Saci_0468	-1.17	39.2	-0.90	43.5	-0.27	-1.21	3.44E-01
VapB2	Saci_1235	0.93	55.3	0.68	55.2	0.25	1.19	2.94E-01
VapC2	Saci_1236	-0.16	46.9	-0.05	49.8	-0.11	-1.08	4.65E-01
VapC3	Saci_1790	-0.75	42.4	-0.63	45.5	-0.12	-1.09	6.24E-01
VapB3	Saci_1791	-0.83	41.8	0.22	51.8	-1.05	-2.07	1.80E-04
VapB4	Saci_1812	1.89	62.6	2.55	69.1	-0.66	-1.58	2.63E-02
VapC4	Saci_1813	2.41	66.6	3.43	75.7	-1.02	-2.03	5.03E-04
VapB5	Saci_1882	-0.54	44.0	0.29	52.3	-0.83	-1.78	8.47E-03
VapC5	Saci_1883	2.35	66.1	2.29	67.1	0.06	1.05	7.85E-01
VapB6	Saci_1952	-1.73	35.0	-0.95	43.1	-0.78	-1.71	4.87E-04
VapC6	Saci_1953	-1.25	38.6	-1.21	41.2	-0.04	-1.03	9.27E-01
VapC7	Saci_1954	2.75	69.2	2.93	71.9	-0.17	-1.13	4.27E-01
VapB7	Saci_1955	1.90	62.7	2.16	66.2	-0.26	-1.20	1.33E-01
VapB8	Saci_1977	2.33	65.9	3.22	74.1	-0.89	-1.86	4.52E-03
VapC8	Saci_1978	1.48	59.5	2.14	66.0	-0.66	-1.58	2.51E-02
VapB9	Saci_1980	0.59	52.7	1.62	62.2	-1.03	-2.04	9.25E-04
VapC9	Saci_1981	-0.13	47.2	0.65	55.0	-0.78	-1.71	1.68E-02
VapB10	Saci_1984	0.57	52.5	1.92	64.4	-1.36	-2.56	1.02E-05
VapC10	Saci_1985	-2.68	27.7	-1.34	40.2	-1.34	-2.53	1.86E-03
VapC11	Saci_2002	2.15	64.5	2.12	65.9	0.03	1.02	8.17E-01
VapB11	Saci_2003	2.72	68.9	3.16	73.6	-0.44	-1.36	1.75E-03
VapB12	Saci_2079	2.92	70.4	3.90	79.1	-0.98	-1.97	2.41E-04
VapC12	Saci_2080	1.08	56.4	0.82	56.2	0.26	1.20	1.69E-01
VapB13	Saci_2166	-0.75	42.5	-1.44	39.5	0.69	1.61	4.41E-02
VapC13	Saci_2167	0.52	52.1	-0.78	44.4	1.30	2.46	4.36E-05
VapC14	Saci_2183	1.18	57.2	0.44	53.4	0.74	1.67	5.73E-04
VapB14	Saci_2184	0.84	54.5	-2.60	30.8	3.44	10.83	3.63E-12
VapC15	Saci_2192	-2.84	26.5	-2.61	30.8	-0.24	-1.18	2.68E-01
VapB15	Saci_2193	1.67	60.9	2.18	66.3	-0.51	-1.42	1.86E-02
Hypothetical protein	Saci_1530	-6.31	0.0	-6.76	0.0	0.45	1.36	2.92E-01
Hypothetical protein	Saci_1138	0.78	54.1	2.63	69.7	-2.71	-6.53	6.48E-12

[a] Microarray data measuring differential expression of genes between biofilm and planktonic cells.

Table 2. *Sulfolobus acidocaldarius* TAfinder Results								
Name	**ID**	**T/A**	**Locus tag**	**Location**	**Length (a.a.)**	**Strand**	**Family**	**Domain**
VapC1	70606299	T	Saci_0467	394110..394478	122	-	PIN-like	cd09981
VapB1	70606300	A	Saci_0468	394465..394713	82	-	RHH-like	COG1753
VapC2	70607005	T	Saci_1236	1052274..1052666	130	+	vapC	-
VapB2	70607004	A	Saci_1235	1052045..1052290	81	+	vapB	-
VapC3	70607519	T	Saci_1790	1557436..1557846	136	-	PIN-like	COG4113
VapB3	70607520	A	Saci_1791	1557834..1558100	88	-	RHH-like	PRK11235
VapC4	70607542	T	Saci_1813	1580918..1581340	140	+	PIN-like	-
VapB4	70607541	A	Saci_1812	1580688..1580921	77	+	RHH-like	-
VapC5	70607611	T	Saci_1883	1677052..1677447	131	+	PIN-like	COG4113
VapB5	70607610	A	Saci_1882	1676838..1677062	74	+	RHH-like	COG3905
VapC6	70607679	T	Saci_1953	1765576..1765995	139	+	vapC	-
VapB6	70607678	A	Saci_1952	1765335..1765583	82	+	vapB	-
VapC7	70607680	T	Saci_1954	1766204..1766599	131	-	PIN-like	cd09872
VapB7	70607681	A	Saci_1955	1766583..1766810	75	-	AbrB-like	COG2002
NA	70607683	T	Saci_1957	1767340..1769043	567	-	-	pfam12568
NA	70607682	A	Saci_1956	1766910..1767353	147	-	-	COG1733
MNT8	70607703	T	Saci_1978	1792029..1792373	114	+	MNT-like	-
HEPN8	70607702	A	Saci_1977	1791620..1792051	143	+	HEPN-like	-
VapC9	70607706	T	Saci_1981	1795579..1795983	134	+	PIN-like	-
VapB9	70607705	A	Saci_1980	1795356..1795592	78	+	RHH-like	-
VapC10	70607710	T	Saci_1985	1799655..1800041	128	+	PIN-like	cd09886
VapB10	70607709	A	Saci_1984	1799411..1799665	84	+	AbrB-like	COG2002
VapC11	70607724	T	Saci_2002	1817055..1817375	106	-	PIN-like	-
VapB11	70607725	A	Saci_2003	1817476..1817742	88	-	RHH-like	-
VapC12	70607797	T	Saci_2080	1898348..1898716	122	+	PIN-like	COG4113
VapB12	70607796	A	Saci_2079	1898115..1898345	76	+	RHH-like	pfam01402
NA	70607828	T	Saci_2111	1932477..1934174	565	+	-	pfam12568
NA	70607829	A	Saci_2112	1934285..1934725	146	+	-	COG1733
VapC13	70607880	T	Saci_2167	2000715..2001335	206	+	vapC	-
VapB13	70607879	A	Saci_2166	2000353..2000703	116	+	vapB	-
VapC14	70607892	T	Saci_2183	2019340..2019957	205	-	vapC	-
VapB14	70607893	A	Saci_2184	2019983..2020327	114	-	vapB	-
VapC15	70607901	T	Saci_2192	2032246..2032686	146	-	PIN-like	-
VapB15	70607902	A	Saci_2193	2032646..2032906	86	-	AbrB-like	-
T/A: This shows the type of the protein. T for Toxin and A for Antitoxin.								
Sequence Name: *Sulfolobus acidocaldarius* DSM 639 chromosome, complete genome								
Length: 2225959 bp								

Table 3. *Sulfolobus acidocaldarius vapBC14* Transcriptional Response to *saci_1223* Deletion									
Gene Product	**Gene ID**	**MW001 Biofilm/Planktonic**		***Δsaci_1223* Biofilm/Planktonic**		**Biofilm *Δsaci_1223*/MW001**		**Planktonic *Δsaci_1223*/MW001**	
		Fold Change	**p-value**	**Fold Change**	**p-value**	**Fold Change**	**p-value**	**Fold Change**	**p-value**
VapC14 Toxin	Saci_2183	1.7	5.73E-04	1.4	2.51E-02	1.4	1.28E-02	1.7	4.02E-04
VapB14 Antitoxin	Saci_2184	10.8	3.63E-12	3.9	6.29E-07	1.0	8.62E-01	2.9	4.10E-05

[a] Microarray data measuring differential expression of genes between biofilm and planktonic cells of the *S.acidocaldarius* MW001 parent and the *Δsaci_1223* mutant.

Table 4. Prevalence of VapC14 Toxin homologs in the Sulfolobales.

Function	Toxin			
Name	VapC14		VapC13	
Protein Accession	WP_011278971.1		WP_011278959.1	
GenBank Accession	AAY81469.1		AAY81457.1	
Organism	**Locus ID/AA% Identity**		**Locus ID/AA% Identity**	
***Sulfolobus acidocaldarius* DSM 639**	Saci_2183	100.00	Saci_2167	63.00
***Acidianus ambivalens* LEI 10**	D1866_09095		51.50	
***Acidianus brierleyi* DSM 1651**				
***Acidianus hospitalis* W1**	Ahos_1667		52.50	
***Acidianus infernus* DSM 3191**				
***Acidianus manzaensis* YN-25**	B6F84_13285		53.73	
***Acidianus sulfidivorans* JP7**	DFR86_00270		53.50	
***Candidatus Acidianus copahuensis* ALE1**	CM19_01545		54.23	
***Candidatus Aramenus sulfurataquae* Az1**	ASUL_08644		62.50	
***Metallosphaera cuprina* Ar-4**	Mcup_1067	56.18	Mcup_1328	39.41
***Metallosphaera hakonensis* HO1-1**	DFR87_00325		39.38	
***Metallosphaera javensis* AS-7**	MjAS7_1675		36.87	
***Metallosphaera prunae* RON 12/II**	DFR88_02270		37.93	
***Metalosphaera sedula* DSM 5348**	Msed_0856		37.37	
***Metallosphaera tengchongensis* Ric-A**	GWK48_00470		41.48	
***Metallosphaera yellowstonensis* MK1**	MetMK1DRAFT_00004880		54.86	
***Saccharolobus caldissimus* JCM32116**	SACC_25450		53.50	
***Saccharolobus shibatae* B12**	J5U23_02119		53.50	
***Saccharolobus solfataricus* P2**	SSO1868		54.00	
***Stygiolobus azoricus* FC6**				
***Sulfodiicoccus acidiphilus* HS-1**	HS1genome_2027		34.03	
***Sulfolobus islandicus* L.D.8.5**	LD85_0694		54.00	
***Sulfuracidifex metallicus* DSM 6482**				
***Sulfuracidifex tepidarius* IC-007**				
***Sulfurisphaera ohwakuensis* TA-1**	D1869_08965		56.22	
***Sulfurisphaera tokodaii* str. 7**	STK_15930		56.22	

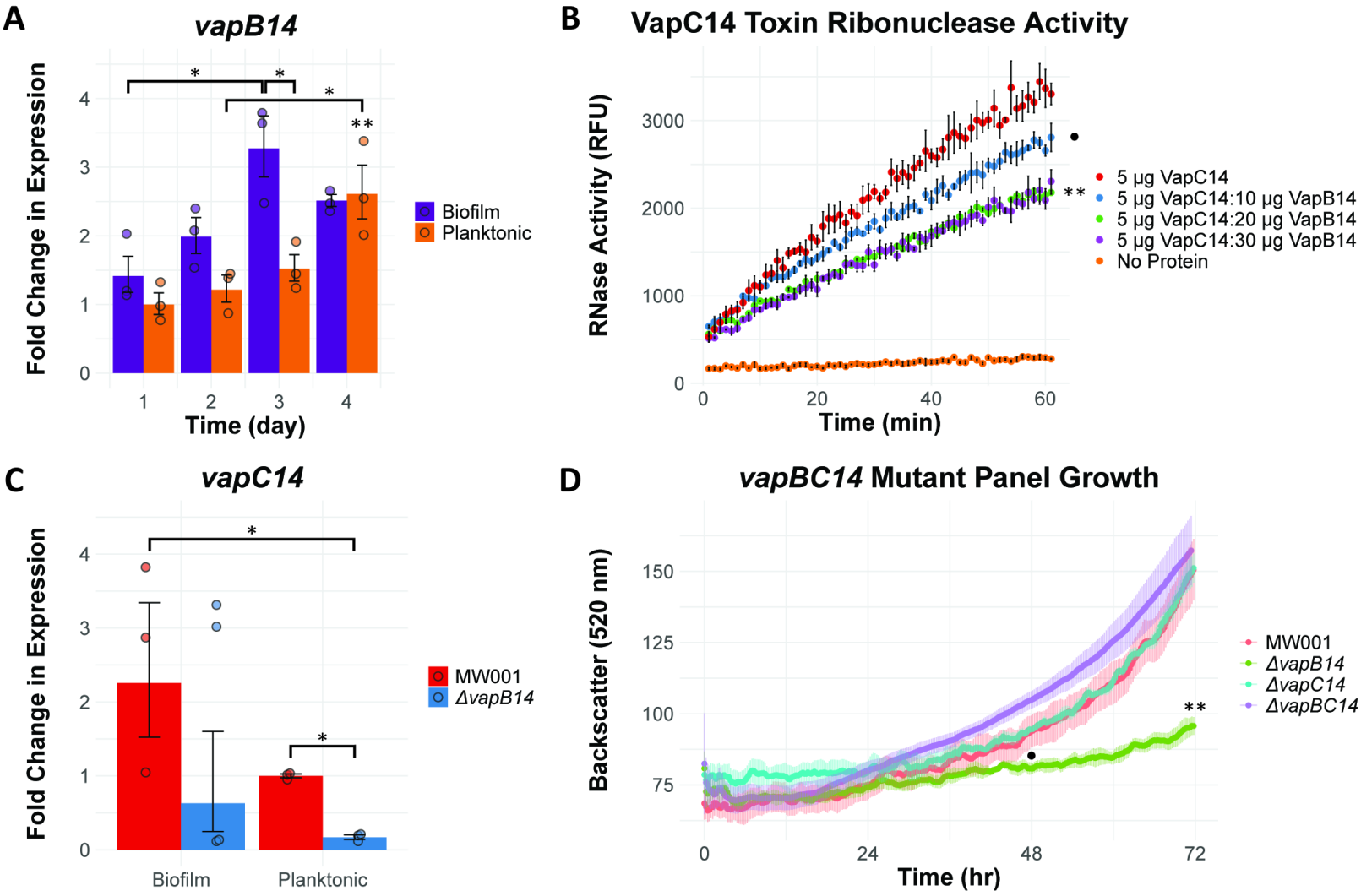
A
vapB14
Fold Change in Expression
Time (day)
Biofilm
Planktonic
B
VapC14 Toxin Ribonuclease Activity
RNase Activity (RFU)
Time (min)
5 µg VapC14
5 µg VapC14:10 µg VapB14
5 µg VapC14:20 µg VapB14
5 µg VapC14:30 µg VapB14
No Protein
C
vapC14
Fold Change in Expression
Biofilm
Planktonic
MW001
ΔvapB14
D
vapBC14 Mutant Panel Growth
Backscatter (520 nm)
Time (hr)
MW001
ΔvapB14
ΔvapC14
ΔvapBC14

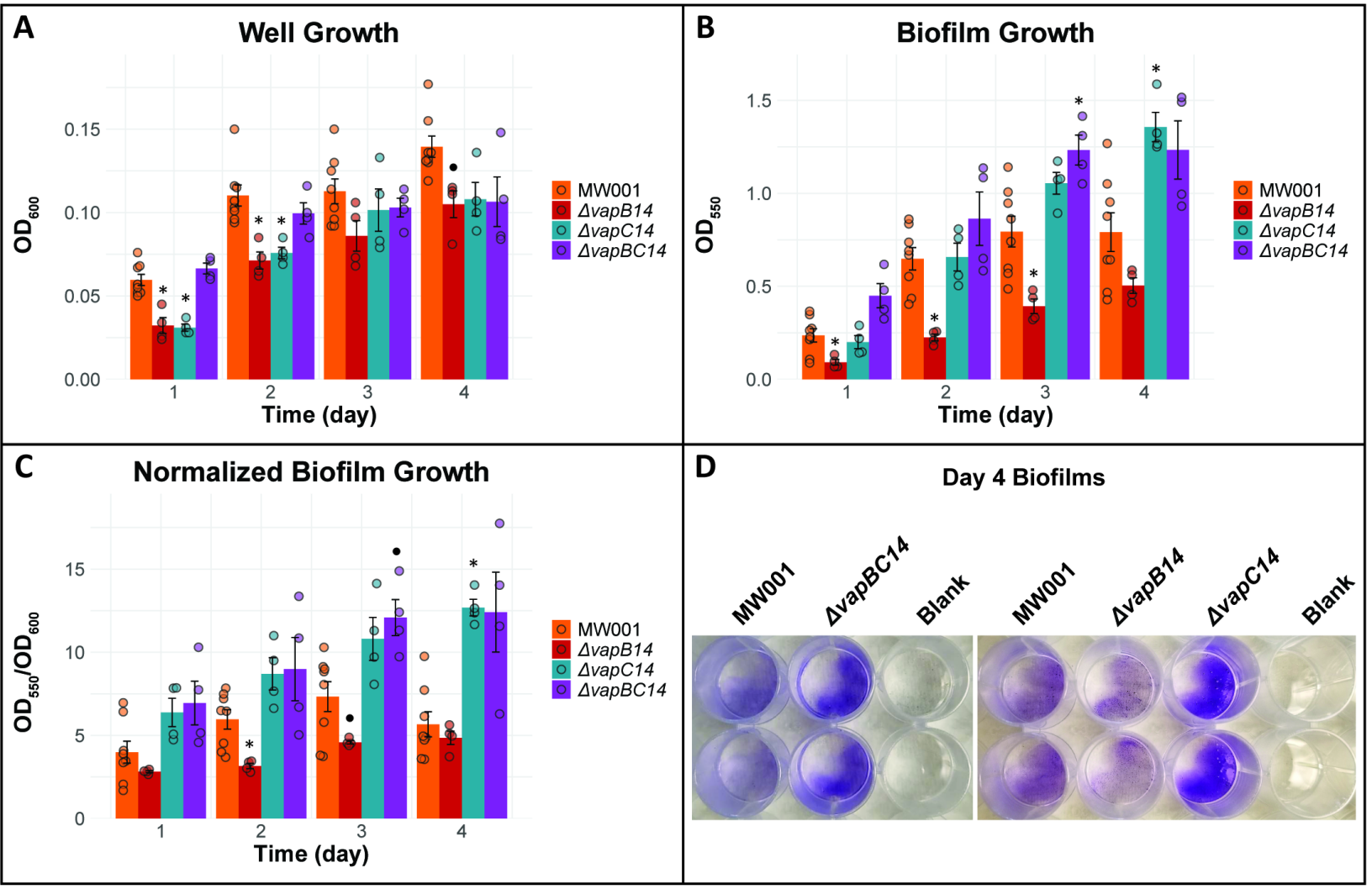
A
Well Growth
OD600
0.15
0.10
0.05
0.00
1
2
3
4
Time (day)
MW001
ΔvapB14
ΔvapC14
ΔvapBC14
B
Biofilm Growth
OD550
1.5
1.0
0.5
0.0
1
2
3
4
Time (day)
MW001
ΔvapB14
ΔvapC14
ΔvapBC14
C
Normalized Biofilm Growth
OD550/OD600
15
10
5
0
1
2
3
4
Time (day)
MW001
ΔvapB14
ΔvapC14
ΔvapBC14
D
Day 4 Biofilms
MW001
ΔvapBC14
Blank
MW001
ΔvapB14
ΔvapC14
Blank

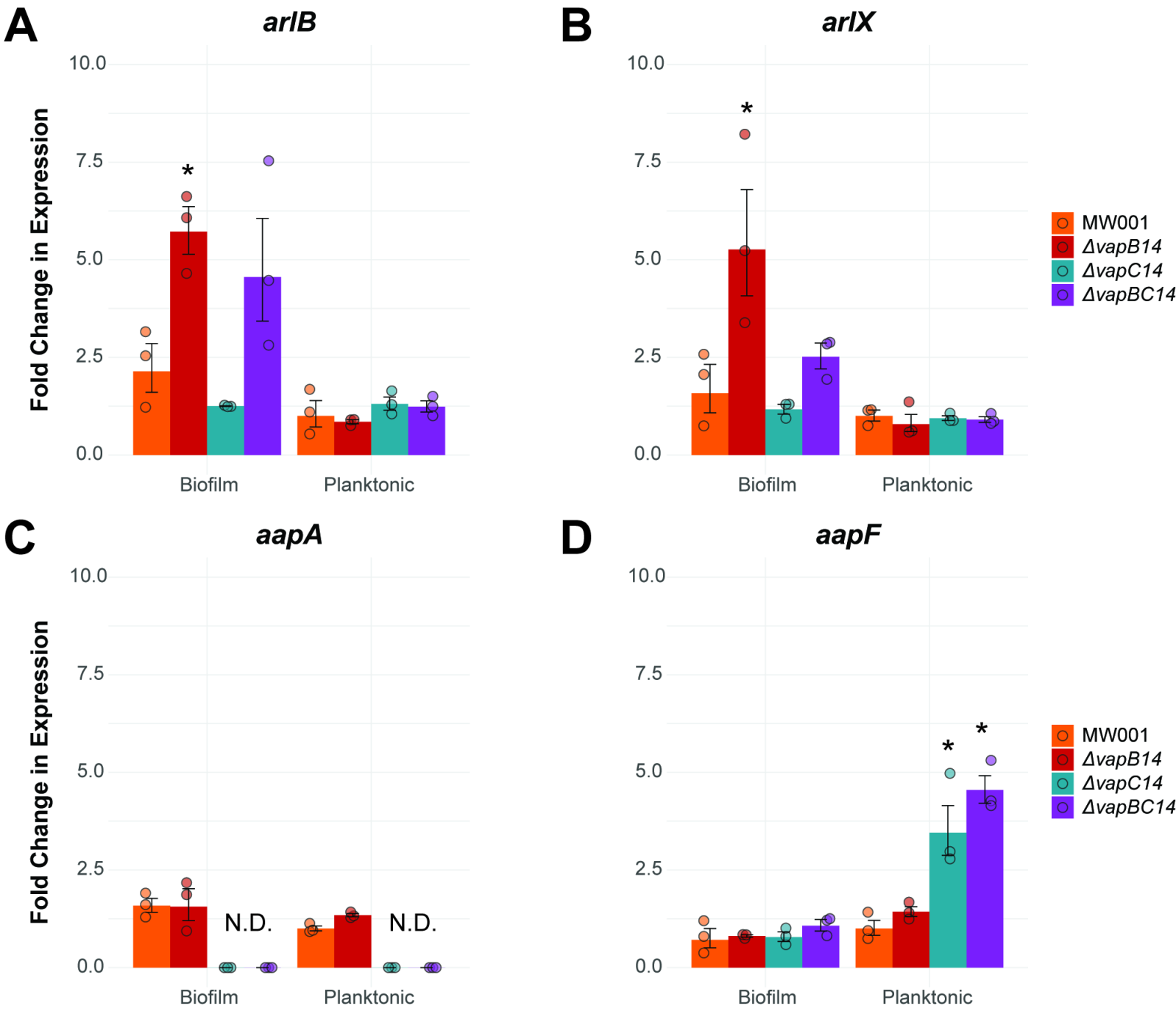
A
arlB
B
arlX
C
aapA
D
aapF
Fold Change in Expression
10.0
7.5
5.0
2.5
0.0
*
N.D.
Biofilm
Planktonic
MW001
ΔvapB14
ΔvapC14
ΔvapBC14

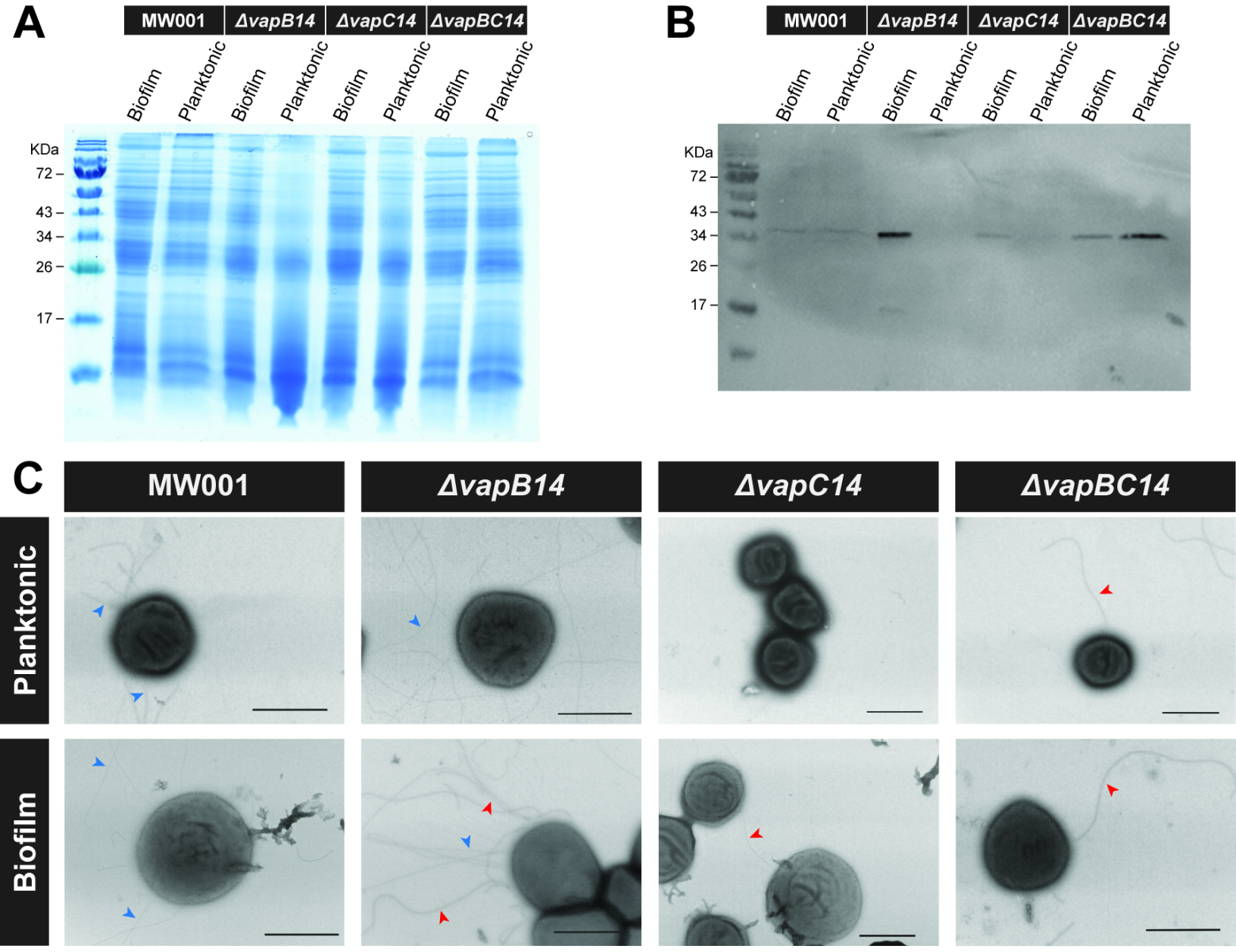
A
MW001
ΔvapB14
ΔvapC14
ΔvapBC14
Biofilm
Planktonic
KDa
72
43
34
26
17
B
C
Planktonic
Biofilm

A **Prevalence of VapB14 Antitoxin homologs in the Sulfolobales**

Function	Antitoxin		
Name	VapB14		
Protein Accession	WP_011278972.1		
GenBank Accession	AAY81470.1		
Organism	Locus ID	% Identity	
		Amino Acid	Nucleotide
Sulfolobus acidocaldarius DSM 639	Saci_2184	100.00	100.00
Acidianus ambivalens LEI 10	D1866_09090	62.28	67.80
Acidianus brierleyi DSM 1651			
Acidianus hospitalis W1	Ahos_1666	72.32	71.74
Acidianus infernus DSM 3191			
Acidianus manzaensis YN-25	B6F84_13280	67.86	72.07
Acidianus sulfidivorans JP7	DFR86_00275	66.97	67.58
Candidatus Acidianus copahuensis ALE1	CM19_01540	70.18	69.18
Candidatus Aramenus sulfurataquae Az1	ASUL_08639	71.05	67.75
Metallosphaera cuprina Ar-4	Mcup_1066	62.50	65.40
Metallosphaera hakonensis HO1-1	DFR87_00770	59.29	67.69
Metallosphaera javensis AS-7	MjAS7_1695	61.95	67.15
Metallosphaera prunae RON 12/II	DFR88_02195	57.39	68.89
Metalosphaera sedula DSM 5348	Msed_0871	57.39	68.89
Metallosphaera tengchongensis Ric-A	GWK48_00265	57.02	
Metallosphaera yellowstonensis MK1	MetMK1DRAFT_00002900	51.79	
	MetMK1DRAFT_00004870	72.32	72.36
Saccharolobus caldissimus JCM32116	SACC_25440	72.32	70.15
Saccharolobus shibatae B12	J5U23_02118	64.04	67.88
Saccharolobus solfataricus P2	SSO1867	67.54	67.48
Stygiolobus azoricus FC6			
Sulfodiicoccus acidiphilus HS-1	HS1genome_2020	57.27	69.30
Sulfolobus islandicus L.D.8.5	LD85_0695	73.21	71.74
Sulfuracidifex metallicus DSM 6482			
Sulfuracidifex tepidarius IC-007	IC007_0597	66.67	70.16
Sulfurisphaera ohwakuensis TA-1	D1869_08970	67.86	72.56
Sulfurisphaera tokodaii str. 7	STK_15940	66.07	72.46

B

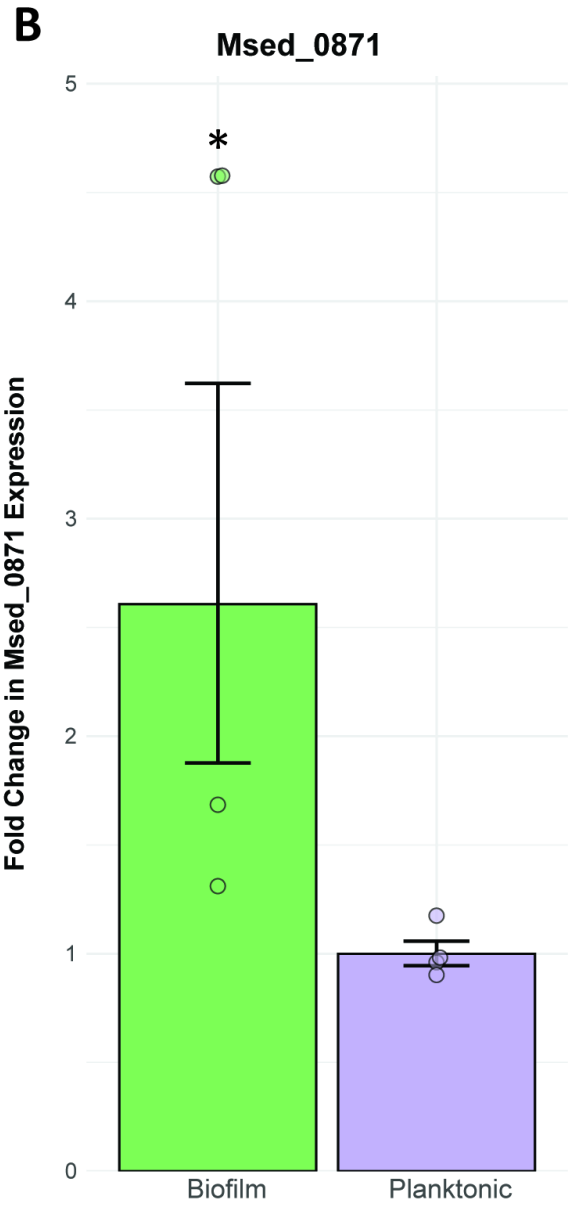

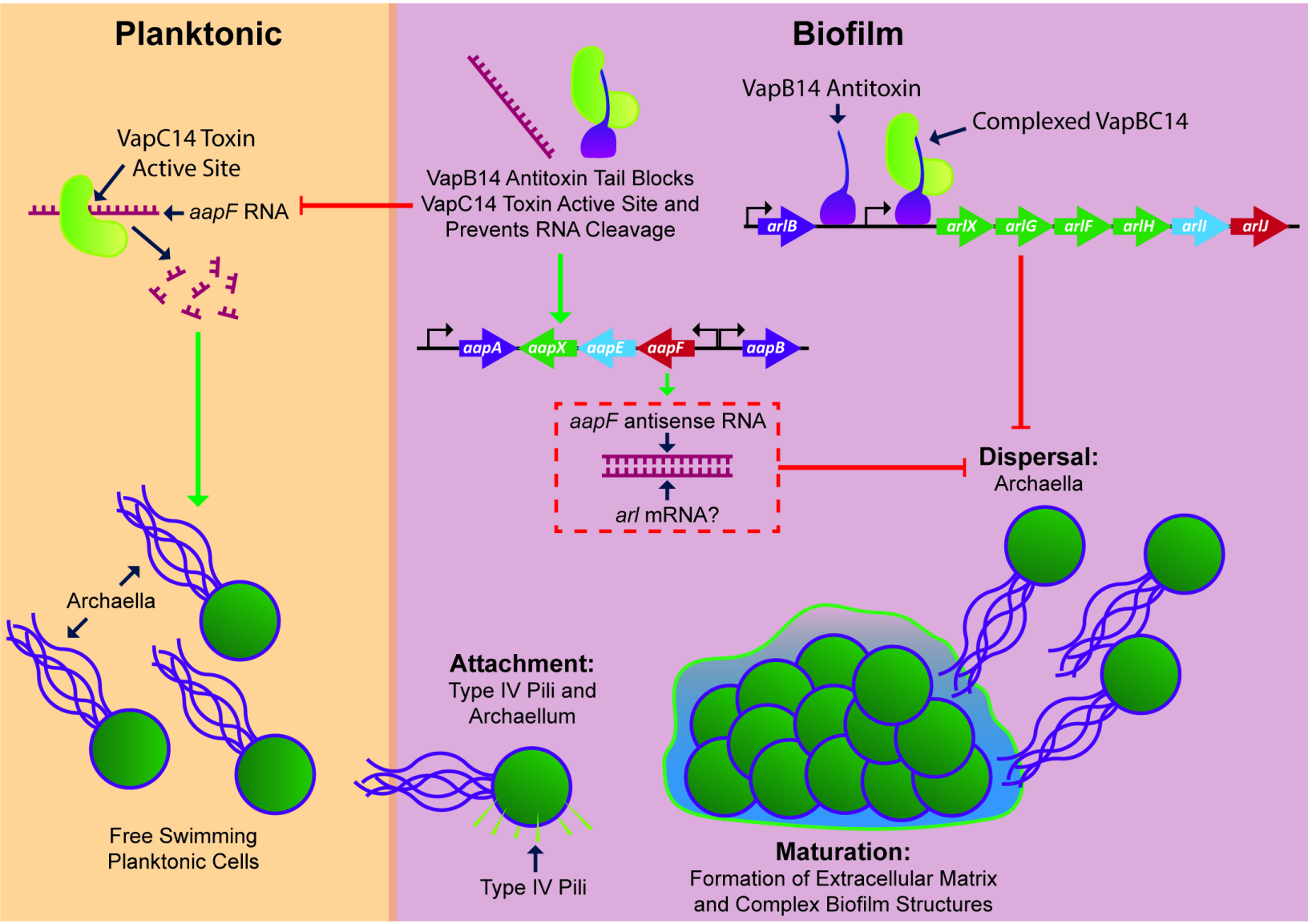
Planktonic
Biofilm
VapC14 Toxin
Active Site
aapF RNA
VapB14 Antitoxin Tail Blocks
VapC14 Toxin Active Site and
Prevents RNA Cleavage
VapB14 Antitoxin
Complexed VapBC14
arlB
arlX
arlG
arlF
arlH
arlI
arlJ
aapA
aapX
aapE
aapF
aapB
aapF antisense RNA
arl mRNA?
Dispersal:
Archaella
Archaella
Free Swimming
Planktonic Cells
Attachment:
Type IV Pili and
Archaellum
Type IV Pili
Maturation:
Formation of Extracellular Matrix
and Complex Biofilm Structures